Engineering Applications

https://publish.mersin.edu.tr/index.php/enap

e-ISSN 2979-9201

Investigation of the effects of different curing conditions and sodium content on the mechanical and durability properties of fly ash based geopolymer mortar with various proportions of silica fume substituted

Ela Bahsude Gorur Avsaroğlu [*1], Mustafa Eken [2], Emre Eser [3]

[1] Department of Construction Technology, Vocational School of Technical Sciences, Sutcu Imam University, Kahramanmaras, TURKEY, ela_gorur@hotmail.com
[2] Construction Technology Department, Elbistan Vocational School, Istiklal University, K.maras/Elbistan, TURKEY, mustafaeken.me@gmail.com
[3] Civil Engineer, Kahramanmaras, TURKEY, emreser1995@gmail.com

Cite this study: Gorur Avsaroglu, E. B., Eken, M. & Eser, E. (2024). Investigation of the effects of varying curing time, temperature and sodium ratio on the mechanical and durability properties of fly ash based geopolymer mortar with different amounts of silica fume substituted. Engineering Applications, 3(3), 226-247.

Keywords
Silica fume
Fly ash
Mechanical and durability properties
Curing time
Temperature
Sodium ratio

Research Article
Received:17.10.2024
Revised:19.10.2024
Accepted:05.12.2024
Published:30.12.2024

Abstract

In this study, F class fly ash-based geopolymer mortar samples with 8%, 10%, and 12% NaOH concentrations were created by replacing 1%, 2%, 3%, 4% and 5% silica fume. Geopolymer mortar samples were thermally cured at 65, 75, and 85 ° C for 24, 48, and 72 hours. Geopolymer mortar samples were subjected to tests for workability, compressive strength, flexural strength, resistance to high temperatures, and abrasion. Geopolymer mortar samples were subjected to a high temperature compressive strength test at 200, 400, 600, 800, and 1000 °C. Mechanical and durability tests conducted on the samples of thermally cured geopolymer mortar indicate that a specific amount of silica fume substitution increases the strength. Additionally, it is observed that the addition of silica fume contributes positively to the machinability. At all concentration ratios, the mortar sample containing 4% silica fume and subjected to thermal curing at 85°C for 72 hours had the highest compressive and flexural strength values. The maximum compressive strength values achieved at high temperature were also obtained in the sample with 4% silica fume substitution. After testing the produced mortar samples, it has been concluded that 4% silica fume substitution based on Class F fly ash is the optimal value.

1. Introduction

In addition to requiring a substantial amount of energy during production, Portland cement emits carbon dioxide [1]. Approximately 8% of the carbon dioxide (CO_2) released into the environment is attributable to the usage of cement in the concrete industry [2]. Carbon emissions released into the environment during cement production are known to cause environmental problems such as the greenhouse effect and add to the environmental burden [3]. Consequently, an environmentally acceptable alternative is needed to reduce carbon emissions from the production of Portland cement. Due to its high strength and durability, alkaline activator-activated geopolymer of aluminosilicate wastes can be considered as an alternative binder material [4].

Geopolymer was first discovered by Joseph Davidovits in 1979. The inorganic geopolymer contains Si-O-Si and Si-O-Al bonds. The three-dimensional mesh and aluminum silicate structure endow the geopolymer with exceptional properties, including great strength and durability [5]. Geopolymers are environmentally friendly due

to their low carbon emissions [6], use of industrial wastes as a binder material [7], medium-high density in terms of physical properties [8], high compressive strength with mechanical properties [9], and low permeability in terms of durability, acid and alkali corrosion resistance[10] and fire resistance [11].

In the production of geopolymers with multiple properties, silica- or silica-alumina-rich pozzolans with binding properties are utilized [13]. This enables the use of fly ash [14], rice husk ash [15], and silica fume [16] in the production of geopolymer concrete, which reduces greenhouse gas emissions by decreasing Portland cement production.

Silica fume (SF), also referred to as micro silica, is a byproduct of melting silicon [17]. Due to its high pozzolanic activity, it is utilized as a cement substitute or as an additive to concrete [18]. With its high SiO_2 content and 0.1-0.5 mm fine structure, it has the potential to be employed as a filler in porous structures to enhance their mechanical and durability features [19]. Additionally, silica fume causes a reaction with calcium compounds of fly ash during the creation of geopolymer reactions. According to [24], the reaction permits the creation of C-S-H gels, which are responsible for the development of the strength and durability features of geopolymer concrete. A limited number of studies have explored the consequences of silica fume exposure, as evidenced by the literature review. Mijasrh et al. [20] investigated the use of silica fume as a mineral additive in the geopolymer produced with palm oil ash in limited studies. In their research, Wang and Zhao [21-22] examined the characteristics of silica fume-doped geopolymers under the effect of flame. According to Duan et al. [23], the mechanical characteristics and microstructure analyses of the fly ash-based silica fume additive were tested using heating-cooling cycles at varying temperatures to which geopolymers are subjected. Some researchers examined the effect of silica fume addition with other minerals [24-28], while others examined the resistance and durability of geopolymers produced with silica fume additive against aggressive waters (acid-sulphate-salt) [29,15,30].

$Ca(OH)_2$ dihydroxylation occurs at temperatures between 400 and 500 °C in concretes made with standard Portland cement. Thermal expansion and contraction at the transition region, known as the interface, cause stresses to emerge. The ensuing strains create cracks and a loss in the strength of the concrete. With the production of severe strength losses and fragmentation in Portland cement, the significance of alternative building materials with great resistance to high temperatures has increased. Geopolymer structure degradation at high temperatures, such as 700-800 °C, is more resistant than Portland cement-based concrete [31]. In contrast to Portland cement concretes, the effect of segregation on geopolymer concrete is stable under high temperatures. Pore pressure development is one of the leading causes of segregation and fragmentation in concrete [32]. Table 1 presents various research from the scientific literature that examine the behavior of geopolymer concretes under the influence of high temperatures.

Table 1.Some of the studies in the literature on geopolymers exposed to high temperatures

Reference	Raw material	Alkaline activator	Exposed temperatures (◦C)	Testing
Guerrieri et al. [33]	slag	Na_2SiO_3 $Ca(OH)_2$	100, 200, 300, 400, 500, 600, 700, 800 and 1200	compressive strength, weight loss, visual inspection
Sudarshan and Ranganath [34]	fly ash	Na_2SiO_3 NaOH	150, 200, 300 and 400	physical observations, compressive strength test, rapid chloride permeability test
Abdulkareem et al. [35]	fly ash	Na_2SiO_3 NaOH	100, 200, 400, 500, 600, 700 and 800	compressive strength, thermal expansion, microstructure analysis
Park et al. [36]	fly ash and slag	Na_2SiO_3 NaOH	200, 400, 600 and 800	compressive strength, microstructure analysis
Saavedra and de Guti´errez [37]	fly ash and slag	Na_2SiO_3 NaOH	300, 500, 700, 900 and 1100	compressive strength, visual inspection, microstructure
Zhang et al. [38]	fly ash	Na_2SiO_3 NaOH	100, 200, 400, 600, 800 and 1000	compressive strength, mass loss, visual inspection, microstructure analysis
Sevinc and Durgun [39]	Non-standart fly ash, waste glass powder and silica fume	Na_2SiO_3 NaOH	85	Fresh and hardened unit weights, UPV, compressive strengths, splitting tensile strengths, XRD andSEM
Zhao et al. [40]	fly ash and slag	Na_2SiO_3 NaOH	100, 200, 400, 500, 600, 700 and 800	compressive strength, flexural strength, mass

				loss, microstructure analysis
Ibraheem et al. [41]	fly ash, slag and quarry rock dust	Na_2SiO_3 NaOH	400 and 800	compressive strength, weight loss, microstructure analysis
Topal et al. [42]	slag	Na_2SiO_3 NaOH	100, 200, 400, 600 and 800	compressive strength, ultrasonic pulse velocity, weight loss, sorption, water absorption, visual inspection, microstructure analysis
Tayeh et al. [43]	fly ash and slag	Na_2SiO_+ NaOH	200, 400, 600 and 800	compressive strength
Kantarci et al. [44]	volcanic tuff	NaOH	100, 300, 500 and 700	compressive strength, visual appearance, water absorption, weight loss, microstructure analysis
Huang et al. [45]	slag, silica fume and quartz powder	K_2CO_3 Na_2SiO_3	200, 400, 600 and 800	compressive strength, visual inspection
Memis, and Bilal [46]	slag, ceramic dust and rice husk ash	Na_2SiO_3 NaOH	300, 450 and 600	compressive strength, mass loss
Turkey et al. [47]	Fly ash and glass powder	KOH	200, 400, 550 and 800	mass loss, cracking, water absorption, and microstructure
Bayrak et al. [48]	Slag-based prepacked aggregate geopolymer, silica fume and rice husk ash		150 °C, 300 °C, and 600 °C	compressive strength, mass loss
Gultekin and Ramyar [49]	pumice-, perlite-, fly ash- and burnt clay	Na_2SiO_3 NaOH	450, 600, 750 and 900	XRD ve SEM, compressive strength

The novelty of this study is to investigate the effects of different ratios of silica fume substitution, activator with different Na concentration, different curing time and different curing temperatures on mechanical and durability properties of fly ash based geopolymer mortar. Within the scope of this research, many parameters were investigated and it was tried to determine the optimum values suitable for waste utilization and geopolymer production. There is a limited number of studies investigating many different parameters together and the effects of these parameters on the strength and durability of geopolymer mortar. In order to contribute to the literature, the effect of high temperature on the behavior of silica fume (SF) substituted fly ash based geopolymer mortars was investigated.

2. Material and Method

2.1. Materials

The fly ash used in this study was obtained from the Adana Ceyhan Sugozu thermal power plant in Turkey. According to the TSE EN 450-1[50] standard, it is categorized as F class (low lime) fly ash since the $SiO_2+Al_2O_3+Fe_2O_3$ content is greater than 70% and the CaO content is less than 10%. The silica fume used in the research in accordance with TS EN 13263-1+A1 [51] was obtained from a private laboratory named Dost Kimya in Istanbul (Turkey). Table 2 lists the chemical composition and physical parameters of the fly ash and silica fume utilized in the investigation. Rilem Cembureau Standard sand conforming to TS EN 196-1 [52] was obtained from Limak Set Cement Inc. in Ankara (Turkey). Table 3 displays the granulometry of standard Rilem sand. The specific gravity and water absorption rate of Rilem sand were found to be 2.61 g/cm^3 and 1.275%, respectively. In the manufacturing of geopolymer, 97% pure NaOH was used as an activator, and tap water was added to the mixture to create a solution. Table 4 contains the chemical constituents of NaOH.

2.2. Mixture preparation, casting and curing

Table 5 lists the mixing ratios utilized in the production of geopolymer mortar samples. Samples of mortar were made from fly ash with 1%, 2%, 3%, 4%, and 5% silica fume substitution. Mortar samples made with five

distinct silica substitution rates and three distinct sodium ratios (8%, 10%, 12%), and, were kept at three distinct curing temperatures (65°C, 75°C, 85 °C) and for three different curing times (24h, 48h, 72h).

2.3. Experimental program

Geopolymer samples with and without silica fume were tested for flexural strength, compressive strength, abrasion resistance, and high temperature testing and SEM analyses were conducted. Every experiment was carried out on a group of three samples and the average of the measured quantity was presented in the manuscript. Figure 1 depicts the preparation and curing of geopolymer samples, as well as the used test system. 40x40x160 mm samples of geopolymer mortar were tested for their flexural strength in line with TS EN 1015-11 [53]. After testing for the flexural strength, the broken halves were used to test for the compressive strength 40x40 mm size. Using a Bohme abrasion device and in line with the TS 2824 EN 1338 [54] standard, the Bohme abrasion resistance was determined. In the high temperature test, geopolymer samples were kept for 60 minutes in furnaces at the relevant high temperatures. After 60 minutes of exposure to high temperatures of 200-400-600-800 and 1000 °C, air and water cooling regimes were applied. After 60 minutes of exposure to the relevant temperature and applying the air cooling regime the samples were removed from the oven and allowed to cool in the laboratory environment. Alternatively, other samples that were subjected to a water cooling regime after 60 minutes of exposure to high temperature, were immersed in the curing pool and cooled. The mechanical, physical, and microstructural properties of samples cooled under two distinct conditions were studied separately.

Table 2. Chemical and physical properties of fly ash and silica fume

Chemical and physical properties	Fly Ash	Silica Fume
SiO_2 (%)	60.81	92.02
Al_2O_3 (%)	19.54	0.54
Fe_2O_3 (%)	7.01	0.94
SO_3 (%)	0.31	0.7
Na_2O (%)	2.43	1.42
CaO (%)	5.07	1.84
Total Na eq. alk, (%)	0,63	0.07
K_2O (%)	2.0	2.2
Ignition Loss	2.20	0.27
Particle Density (kg/m^3)	2390	2400
Blaine Specific Surface (cm^2/gr)	4200	200000

Table 3. CEN standard sand sieve analysis and limit values

Property	Sieve Diameter (mm)					
	2.00	1.60	1.00	0.50	0.16	0.08
Sieve Remainder (%)	0.0	7.1	34.6	71.2	86.4	99.3
TS EN 196-1 Limit Values (%)	0	7±5	33±5	67±5	87±5	99±1

Table 4. Chemical Composition of NaOH

Chemical Name	Sodium Hydroxide
Chemical Formula	NaOH
Molecular Weight	40.00 g/mol
Asymmetric	≥97
Na_2CO_3	≤1
Cl	≤0.01
SO_4	≤0.01
Heavy Metal	≤0.002
Al	≤0.002
Fe	≤0.002

Table 5 . Properties of groups

Group-NaOH Concentration	Fly Ash (gr)	Silica Fume (gr)	Sand (gr)	Water (gr)	NaOH (Molarity)	Cure condition (temperature and curing time)
R- 8M	450	-	1350	140	8M	
S1-8M	445.5	4.5	1350	140	8M	
S2-8M	441	9.0	1350	140	8M	
S3-8M	436.5	13.5	1350	140	8M	65 °C-24 h
S4-8M	432	18.0	1350	140	8M	65 °C-48 h
S5-8M	427.5	22.5	1350	140	8M	65 °C-72 h
R- 10M	450	-	1350	140	10M	

S1-10M	445.5	4.5	1350	140	10M	75 °C-24 h
S2-10M	441	9.0	1350	140	10M	75 °C-48 h
S3-10M	436.5	13.5	1350	140	10M	75 °C-72 h
S4-10M	432	18.0	1350	140	10M	
S5-10M	427.5	22.5	1350	140	10M	85 °C-24 h
R- 12M	450	-	1350	140	12M	85 °C-48 h
S1-12M	445.5	4.5	1350	140	12M	85 °C-72 h
S2-12M	441	9.0	1350	140	12M	
S3-12M	436.5	13.5	1350	140	12M	
S4-12M	432	18.0	1350	140	12M	
S5-12M	427.5	22.5	1350	140	12M	

Figure 1. Geopolymer production and testing system

3. Results and discussion

3.1. Workability Test

For the workability spreading test, mortar sample groups with 8, 10, and 12M NaOH concentrations were prepared, and the test results found according to TS EN 1015-3 [55] are depicted in Figure 2 in the form of a bar graph. The differences of the workability values being too little, numerical values will be presented below for the purpose of close checks by the readers.

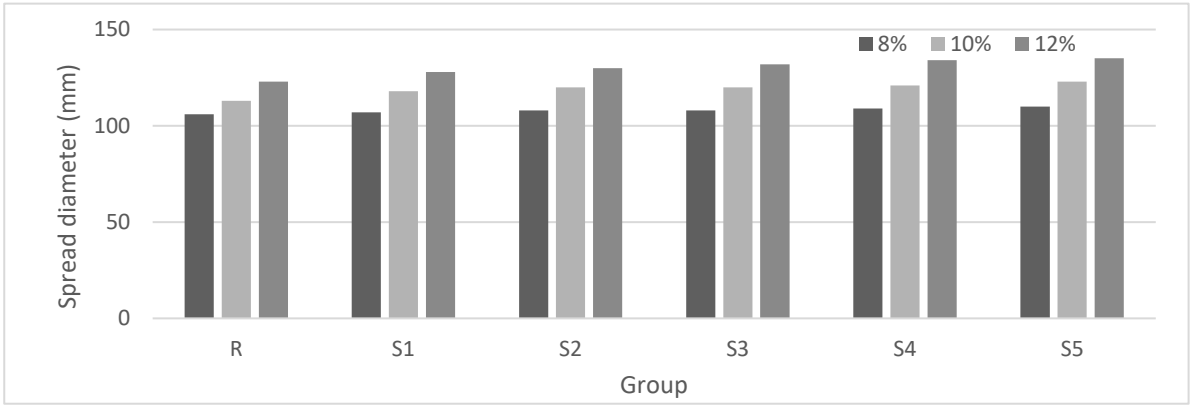

Figure 2. Workability values of fresh mortar groups

It is observed that the reference groups with 8,10, and 12M of sodium hydroxide have workability values of 106, 113, and 123 mm, respectively. Furthermore, the corresponding values for mortar groups containing 1% silica fume are 107, 118, and 128 mm, those for 2% silica fume are 108, 120, and 130 mm, those for 3% silica fume are 108, 120, and 132 mm, those for 4% silica fume are 109, 121, and 134 mm, and those for 5% silica fume are 110, 123, and 135 mm, respectively. Workability values of the reference group and the silica fume added ones reveals that the workability increases as the silica fume additive and alkali activator ratio increase. Dehghani et al.[85] reported that fluidity depends on the SiO_2/Al_2O_3 ratio. It is realized that the + ions surrounding the ash particles boost the workability of the fly ash-based mortar samples when silica fume is added. With a surplus of + ions, workability increases. The results of this study are consistent with those of previous research [56-58].

3.2. Compressive strength

Figure 3 depicts the compressive strength values of groups with varying silica fume additive rates, cured at different temperatures for different curing times.

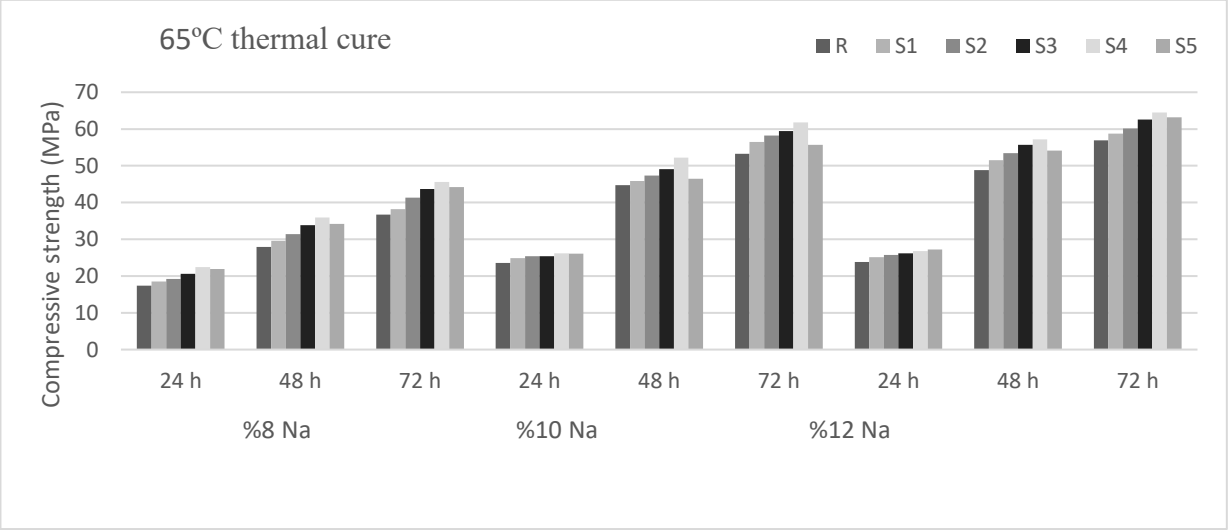

***Na** - sodium hydroxide

(a)

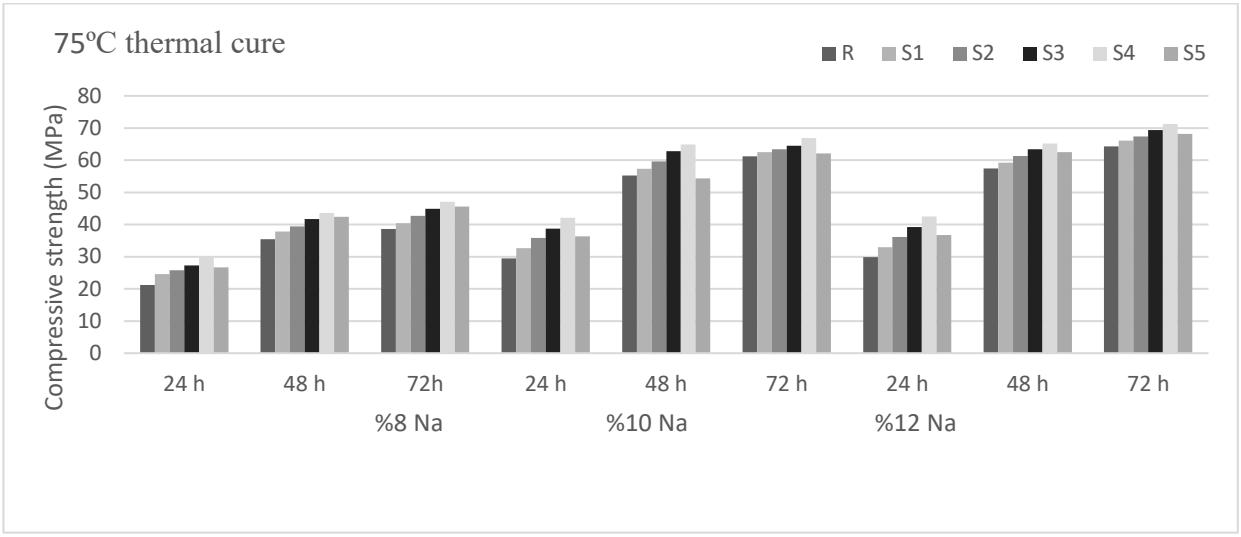

(b)

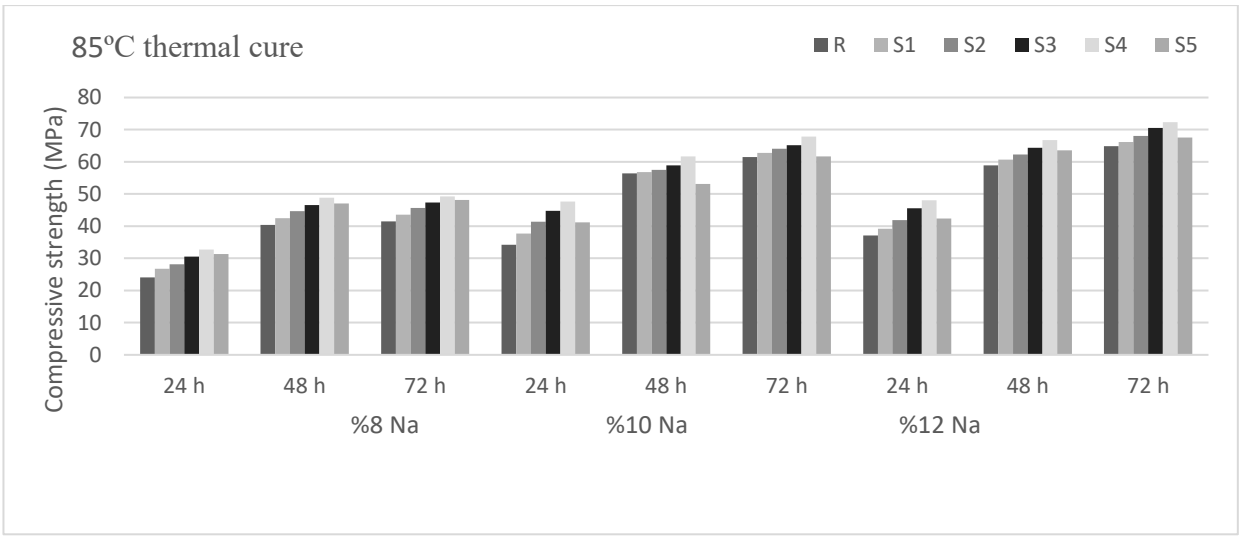

(c)

Figure 3. Compressive strengths of groups cured at 65°C (a), 75°C (b), and 85°C (c)

Compressive strengths of groups cured at 65°C reveals that the compressive strength rises with increasing curing time and NaOH concentration. Among S4 groups with 8M, 10M, and 12M concentrations, the ones cured for 72 hours had the maximum strengths of 45.6MPa, 61.8MPa, and 64.5MPa, respectively. Among the groups with 8M, 10M, and 12M concentrations, S4 groups had the highest compressive strengths after 24 hours, 48 hours, and 72 hours of curing, while the reference group had the lowest compressive strength. Among all groups with 8M, 10M, and 12M concentrations, the reference ones cured for 24 hours had the lowest compressive strength, with the values of 17.4MPa, 23.6MPa, and 23.8MPa, respectively. For all curing times and silica concentrations, the compressive strengths of all silica-substituted groups were higher than those of the reference ones. However, in all cases considered, the compressive strengths of S5 groups are lower than those of S4 groups. This means that increasing the silica concentration above 4% causes a decrease in the compressive strengths of groups cured at 65°C.

Compressive strengths of groups cured at 75°C reveals that the compressive strength rises with increasing curing time and NaOH concentration. Among S4 groups with 8M, 10M, and 12M concentrations, the ones cured for 72 hours had the maximum strengths of 47.1MPa, 66.9MPa, and 71.3MPa, respectively. Among the groups with 8M, 10M, and 12M concentrations, S4 groups had the highest compressive strength after 24 hours, 48 hours, and 72 hours of curing, while the reference group had the lowest compressive strength. Among all groups with 8M, 10M, and 12M concentrations, the reference ones cured for 24 hours had the lowest compressive strengths, with the values of 21,2MPa, 29,5MPa, and 29,9MPa, respectively. For all curing times and silica concentrations, the compressive strengths of all silica-substituted groups were higher than those of the reference ones. However, in all cases considered, the compressive strengths of S5 groups are lower than those of S4 groups. This means that increasing the silica concentration above 4% causes a decrease in the compressive strengths of groups cured at 75°C.

Compressive strengths of groups cured at 85°C reveals that the compressive strength rises with increasing curing time and NaOH concentration. Among S4 groups with 8M, 10M, and 12M concentrations, the ones cured for 72 hours had the maximum strengths of 49,3MPa, 67,9MPa, and 72,3MPa, respectively. Among the groups with 8M, 10M, and 12M concentrations, S4 groups had the highest compressive strength after 24 hours, 48 hours, and 72 hours of curing, while the reference group had the lowest compressive strength. Among all groups with 8M, 10M, and 12M concentrations, the reference ones cured for 24 hours had the lowest compressive strengths, with the values of 24,1MPa, 34,2MPa, and 37,1 MPa, respectively. For all curing times and silica concentrations, the compressive strengths of all silica-substituted groups were higher than those of the reference ones. However, in all cases considered, the compressive strengths of S5 groups are lower than those of S4 groups. This means that increasing the silica concentration above 4% causes a decrease in the compressive strengths of groups cured at 85°C.

The addition of silica fume during the production of fly ash-based geopolymer enhances the compressive strength of all series. After 72 hours of curing for a 12M concentration, the sample S4 with the 12M concentration had the highest compressive strength, which was 11.50% higher than the reference sample. In their investigation, Anuar et al. [59] determined the compressive strength values of samples at the ages of 3, 7, 14, 21 and 28 days produced with 8M and 14M sodium hydroxide. Their results showed that the 14M samples had a higher compressive strength than the 8M samples. In the present investigation, the samples with 12M silica concentration had the highest compressive strength, which was supported by previous research. Other authors mentioned that the use of alkaline solution of sodium hydroxide had a good effect on geopolymerization, depending on the pH level rise and the controlled hydration activity [60]. In all series of the investigation, the increase in the compressive strength value by silica fume addition can be explained by the pozzolanic activity of silica fume. Silica fume, which possesses highly reactive pozzolanic characteristics, enables gel development, resulting in increased compressive strength. This explanation also incorporates corroborating results from previous studies [23]. In addition, the extremely fine structure of silica fume causes a micro-filling effect in the matrix phase of substituted mixes. Consequently, it renders a stronger and denser microstructure [30]. Furthermore, the addition of silica fume results in an increase in concentration, while the rise in molarity contributes to a better dissolution of aluminosilicate sources, thus, enhancing the geopolymer formation process [61-62]. However, it was observed that the change in pressure first increased and then decreased with the SiO_2/Al_2O_3 ratio [87]. The addition of silica fume to the S4 sample with 12M concentration raised the SiO_2/Al_2O_3 ratio, and the increase in silicate ions caused a considerable increase in strength values [30]. It is thought that in silica substitutes above 4%, the amount of extra silica that cannot react negatively affects the strength at all ages and temperatures [63].

3.3. Flexural strength

Figure 4 depicts the flexural strength values of fly ash-based groups with varying silica fume additive rates, cured at different temperatures for different curing times.

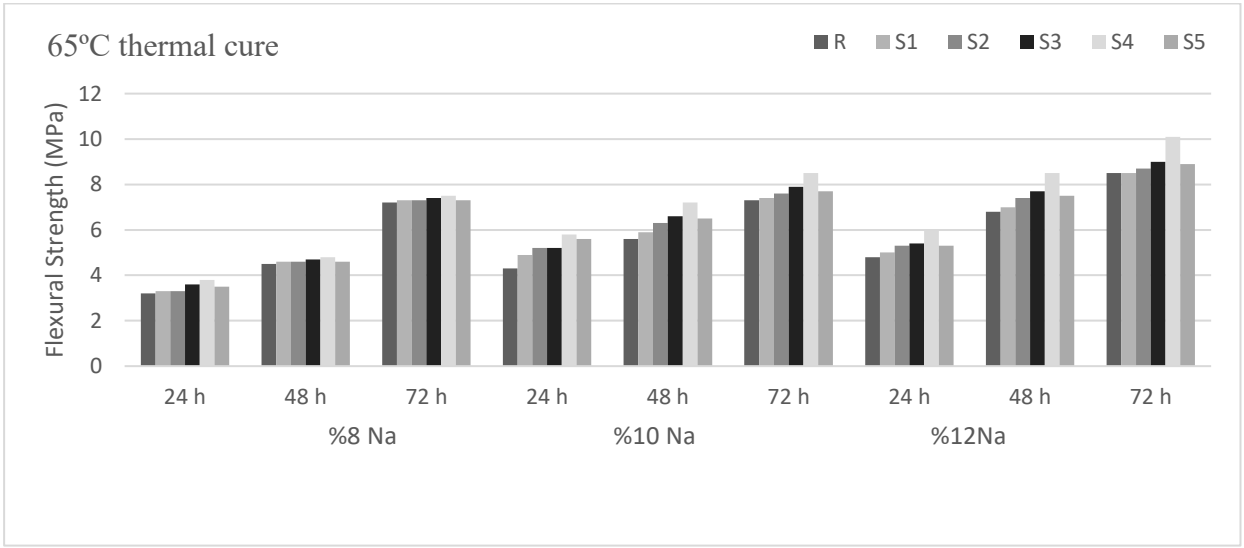

*__Na -__ sodium hydroxide
(a)

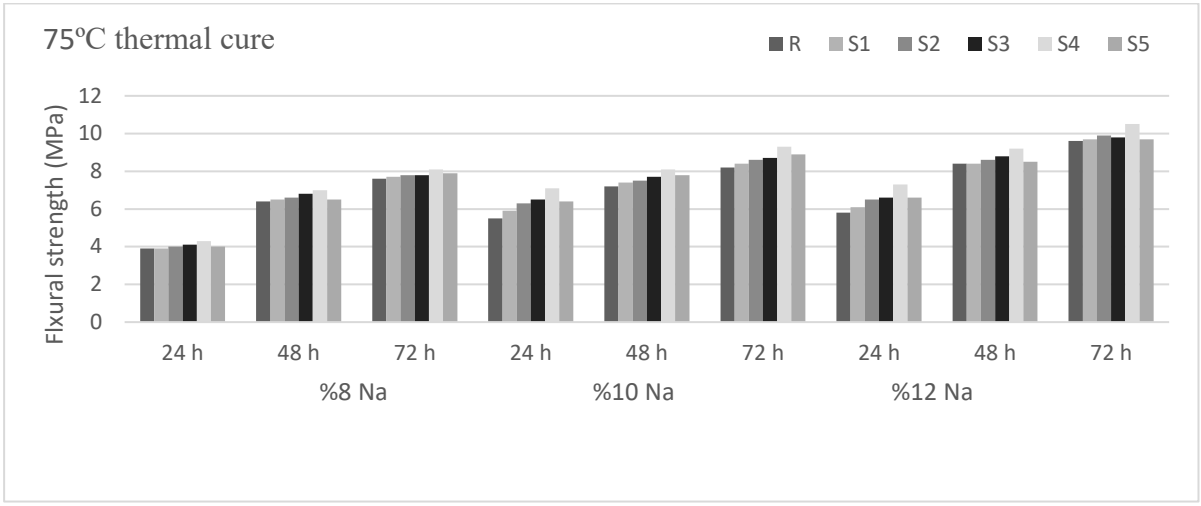

(b)

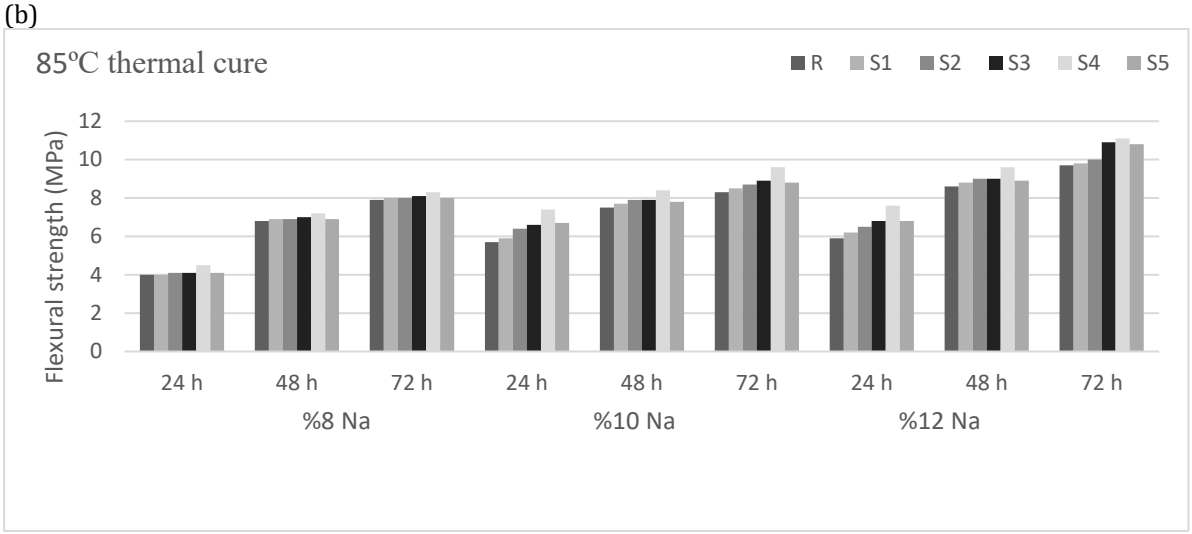

c)

Figure 4. Flexural strengths of groups cured at 65°C (a), 75°C (b), and 85°C (c)

Flexure strength data of groups cured at 65°C reveals that the flexure strength increases with increasing curing time and NaOH concentration. Among S4 groups with 8M, 10M, and 12M concentrations, the ones cured for 72 hours had the maximum strengths of 7.5MPa, 8.5MPa, and 10.1MPa, respectively. Among the groups with 8M, 10M, and 12M concentrations, S4 groups had the highest flexural strengths after 24 hours, 48 hours, and 72 hours of curing, while the reference sample had the lowest flexural strength. Among all groups with 8M, 10M, and 12M concentrations, the reference ones cured for 24 hours had the lowest strength, with the values of 3.2MPa, 4.3MPa, and 4.8MPa, respectively. For all curing times and silica concentrations, the flexural strengths of all silica-substituted groups were higher than those of the reference ones. However, in all cases considered, the flexure strengths of S5 groups are lower than those of S4 groups. This means that increasing the silica concentration above 4% causes a decrease in the flexure strengths of groups cured at 65°C.

Flexure strength data of groups cured at 75°C reveals that the flexural strength increases with increasing curing time and NaOH concentration. Among S4 groups with 8M, 10M, and 12M concentrations, the ones cured for 72 hours had the maximum flexural strengths of 8.1MPa, 9.3MPa, and 10.5MPa, respectively. Among the groups with 8M, 10M, and 12M concentrations, S4 groups had the highest flexural strengths after 24 hours, 48 hours, and 72 hours of curing, while the reference group had the lowest flexural strength. Among all groups with 8M, 10M, and 12M concentrations, the reference ones cured for 24 hours had the lowest flexure strength, with the values of 3.9MPa, 5.5MPa, and 5.8MPa, respectively. For all curing times and silica concentrations, the flexural strengths of all silica-substituted groups were higher than those of the reference ones. However, in all cases considered, the flexural strengths of S5 groups are lower than those of S4 groups. This means that increasing the silica concentration above 4% causes a decrease in the flexural strengths of groups cured at 75°C.

Flexural strength data of groups cured at 85°C reveals that the flexural strength increases with increasing curing time and NaOH concentration. Among S4 groups with 8M, 10M, and 12M concentrations, the ones cured for 72 hours had the maximum flexural strengths of 8.3MPa, 9.6MPa, and 11.1MPa, respectively. Among the groups with 8M, 10M, and 12M concentrations, S4 groups had the highest flexural strengths after 24 hours, 48 hours, and 72 hours of curing, while the reference group had the lowest flexural strength. Among all groups with 8M, 10M,

and 12M concentrations, the reference sample cured for 24 hours had the lowest flexural strength, with the values of 4.0MPa, 5.7MPa, and 5.9MPa, respectively. For all curing times and silica concentrations, the flexural strengths of all silica-substituted groups were higher than those of the reference ones. However, in all cases considered, the flexural strengths of S5 groups are lower than those of S4 groups. This means that increasing the silica concentration above 4% causes a decrease in the flexural strengths of groups cured at 85°C.

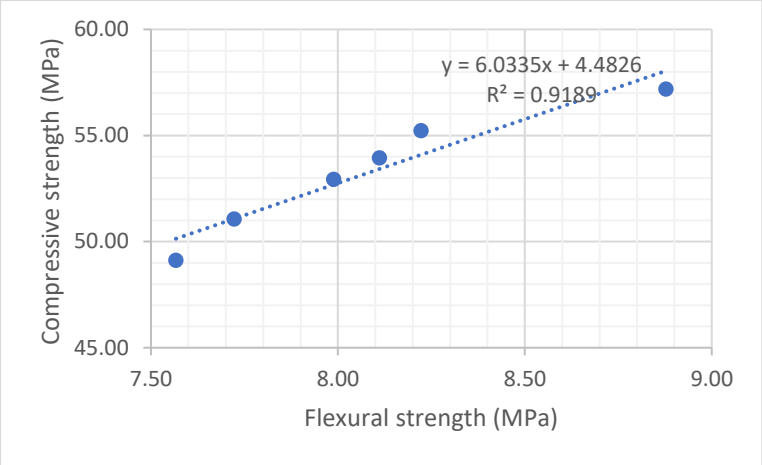

Figure 5. The relationship between the flexural strength and compressive strength values of geopolymer mortars

Similar results were obtained for flexural and compressive strength values (Fig. 5). Among groups with 8M concentration, S4 group cured for 72 hours exhibited the highest increase in flexural strength with 19% over the reference group. Each of the other silica-added groups had the following flexural strength increase rates compared to the reference group, S1 5%, S2 9%, S3 14%, and S5 16%. Among groups with 10M concentration, S4 group cured for 72 hours exhibited the highest increase in flexural strength with 15.70% increase in flexural strength compared to the reference group. The other silica-added groups had higher flexural strengths than the reference sample, with increase rates of S1 2.5%, S2 4.92%, S3 7.30%, and S5 6.10%. Among groups with 12M concentration, S4 group cured for 72 hours exhibited the highest increase in flexural strength with 14.50% increase in flexural strength compared to the reference group. In comparison to the reference sample, the flexural strengths of the other silica-added samples had the following increase rates, S1 1.1%, S2 3.3%, S3 12.4%, and S5 11.40%. Flexural strength values of groups with 12M concentration cured for 72 hours at 85°C are in the range 9.7-11.1 MPa. lkentapar and Ozsoy [63] produced geopolymer samples with 8M, 10M, and 12M NaOH concentrations cured at two distinct temperatures, 60°C and 90°C, for 24h, 48h, and 72h and found flexural strength values in the range 5.7-11.8MPa. The results of the present study and the results of reference [63] look perfectly consistent with each other. It has also been noted by other authors that the high amorphous silica content in the structure of geopolymers including silica fume as a substitute contributes positively to the strength, durability, and microstructure properties of mortars and improves their geopolymeric structure [30,64-65].

3.4. Determining Abrasion Resistance

At the end of the 72 hours of thermal curing at 85°C, cubic geopolymer samples of 71x71x71 mm dimensions were removed from the oven and allowed to cool at room temperature. After determining their weights and volumes, they were abraded in line with TS 2824 EN 1338 [54] with a Bohme device and their weight and volume losses were determined.

Table 6. Abrasion resistance of mortar groups (12M-72h-85°C)

Group	Volumetric loss ($mm^3/5000mm^2$)	Weight loss (gr)
R	3925	8.62
S1	3844	8.39
S2	3709	8.09
S3	3511	7.74
S4	3348	7.38
S5	3402	7.41

Table 6 provides the abrasion resistance properties, via the volumetric and weight loss values, of mortar groups produced with 12M concentration and 72 h curing time at 85°C. High volumetric and weight loss values indicate that the abrasion resistance of a sample is low, whereas low volumetric loss and weight loss values indicate that the abrasion resistance of a sample is high. The sample with the greatest volumetric and weight loss among the

geopolymer groups was the reference group, whereas the group with the least volumetric and weight loss was group S4. The groups containing silica fume exhibited greater resistance to weight loss due to abrasion than the control group by the following percentages: S1-2.8%, S2-6.6%, S3-11.4%, S4-16.9%, and S5-16.4%. The micro-filling effect of silica fume with its tiny particles can explain the positive effect of it on enhancing the abrasion resistance of samples. It has been stated previously in the literature that the adhesion and abrasion properties of geopolymers are superior to those of cement-based repair materials [66]. In addition, several researchers have proven in the literature [67-69] that there is a correlation between abrasion resistance and compressive strength values, i.e. samples with high compressive strength values also have high abrasion resistance. It was suggested that a similar association existed in samples containing silica fume.

3.5. Compressive Strength Following Exposure to High Temperatures

Figure 6 depicts the compressive strength values of samples with concentrations of 8M, 10M, and 12M cured for 72 hours at 85°C before and after the fire test.

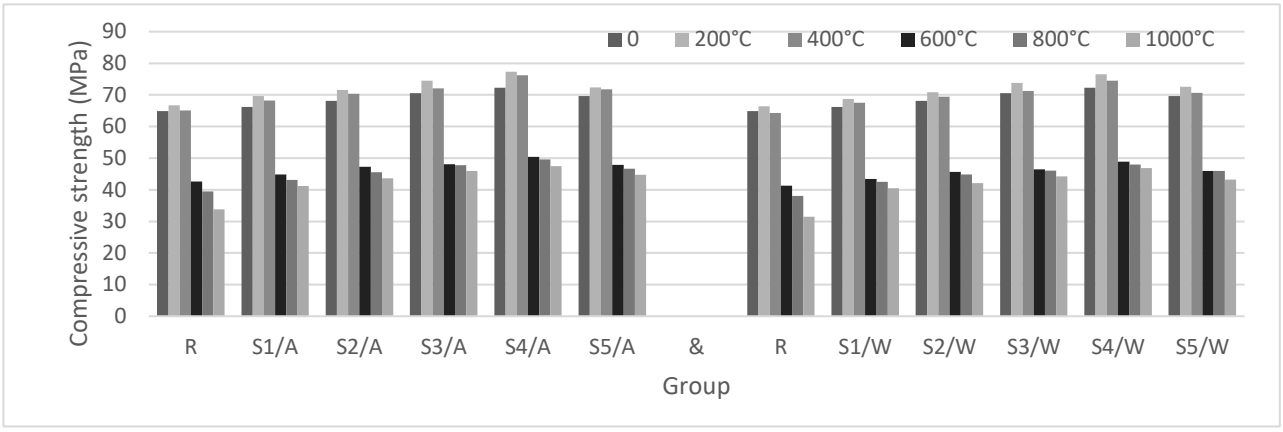

(a)

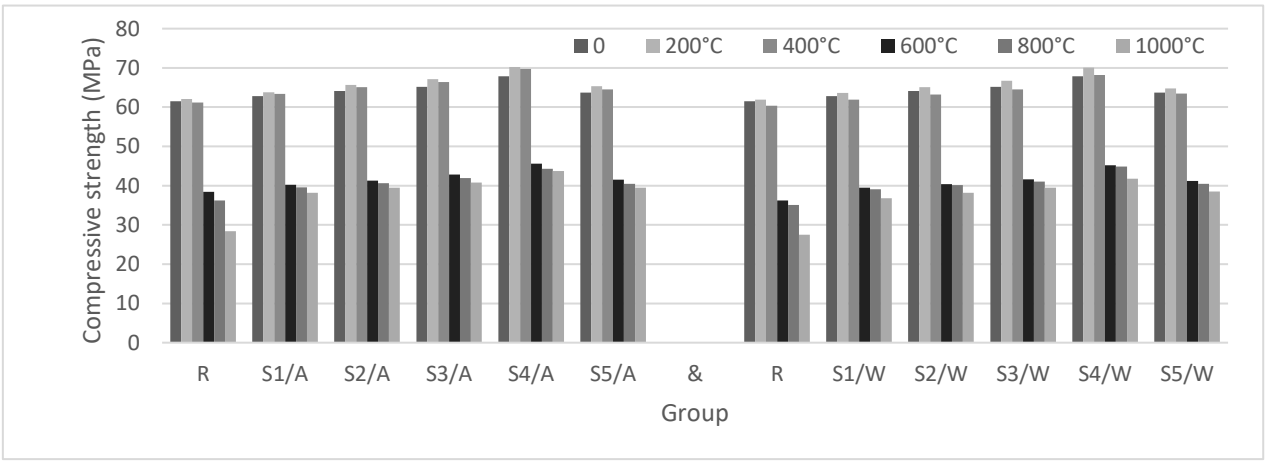

(b)

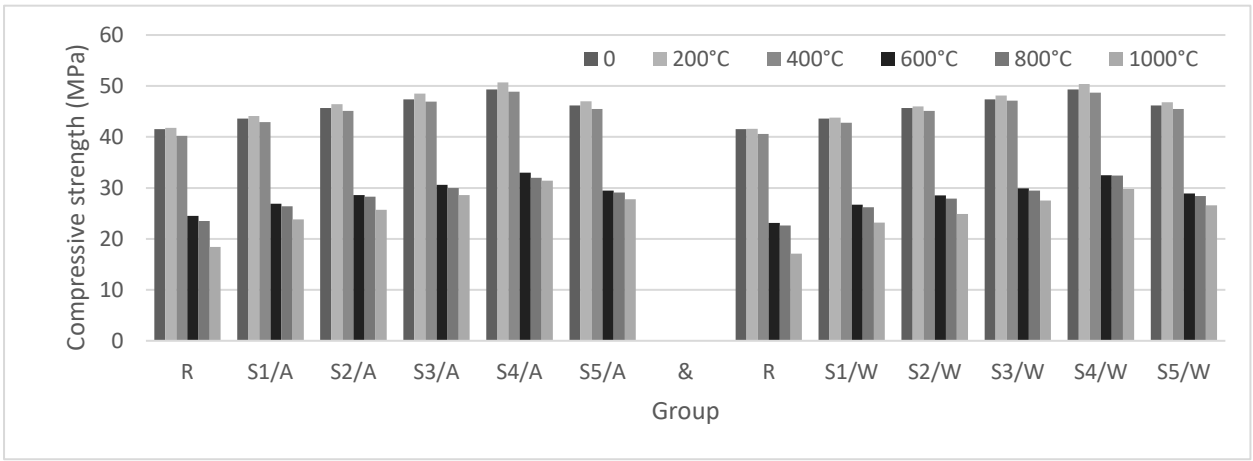

(c)

Figure 6. Residual compressive strengths of groups after fire test (a) 8M concentration (b) 10M concentration (c) 12M concentration

The fire test was carried out on each group and with each of the three 8M, 10M, and 12M concentration values after having been cured for 72 hours at 85°C. The compressive strength values of all groups, were determined after exposure to high temperatures of 200°C, 400°C, 600°C, 800°C, and 1000°C followed by a cooling regime in air and water, each at a time.

After the 8M concentration groups were exposed to the high temperature of 200°C, the groups cooled in air experienced increases of 1.1-2.8% in the compressive strength compared to the reference one, while the compressive strengths of the groups cooled in water increased by 0.5-2.2%. Considering the two alternative cooling regimes after the application of 200°C, the greatest improvement in compressive strength was produced in S4 group with the air cooling regime. Anyhow, for 200°C, the compressive strength of all groups increased in both cooling regimes. The compressive strength of any group cooled in air was found to be greater than that of the same group with the same concentration and the same high temperature cooled in water. For 400°C and higher temperatures, compressive strength losses were detected in both cooling regimes for all groups. For 400, 600, 800, and 1000°C, groups cooled in air exhibited compressive strength losses of 0.8-1.6%, 49.4-62.1%, 54.1-65.2%, and 57.1-83.2%, respectively, whereas the losses for cooling in water were 1.2-1.9%, 51.7-63.3%, 56.1-66.4%, and 65.4-87.9%, respectively.

After the 10M concentration groups were exposed to the high temperature of 200°C, the groups cooled in air experienced increases of 1.6-3.3% in the compressive strength compared to the reference one, but the compressive strength of the groups cooled in water increased by 1.3-3.1%. Anyhow, for 200°C, the compressive strength of all groups increased in both cooling regimes. The compressive strength of any group chilled in air was found to be greater than that of the same group with the same concentration and the same high temperature cooled in water. In groups heated to 400°C, it was observed that the ones cooled in air had a compressive strength increase of 0.9% to 2.6% for all groups containing silica fume, but the control group experienced a pressure loss of 0.5%. In addition, groups chilled in water after the application of 400 °C exhibited a compressive strength drop between 0.3% and 1.5%. It was noted that the compressive strength loss of groups cooled in air after 600°C, 800°, and 1000°C were in the ranges 48.9-56.2%, 53.3-58.6%, and 55.4-64.4%, respectively. In contrast, the water-cooled groups experienced compressive strength losses of 50.2-59.1%, 51.2-60.6%, and 62.4-70.7%, respectively.

After the 12M concentration groups were exposed to the high temperature of 200°C, the groups cooled in air experienced increases of 4.2-13.7% in the compressive strength compared to the reference one, while the compressive strength values of the groups cooled in water increased by 3.65 to 5.55%. Considering the two alternative cooling regimes after the application of 200°C, the greatest improvement in compressive strength was produced in S4 group with the air cooling regime. Anyhow, for 200°C, the compressive strength of all groups increased in both cooling regimes. The compressive strength of any group cooled in air was found to be greater than that of the same group with the same concentration and the same high temperature cooled in water. In groups heated to 400°C, it was observed that in all groups with silica fume, there were increases in the ones cooled in air, in the range 2.9% to 5.1%, whereas in the ones cooled in water, in the range 1.9% to 3.0%, and a loss of 0.9% took place in the reference group. It was noted that the compressive strength loss in groups cooled in air after 600°C, 800°, and 1000°C were in the ranges 43.5-47.8%, 45.8-53.6%, and 52.2-60.7%, respectively, whereas in groups cooled in water, in the ranges 47.9-52.5%, 50.6-55.8%, and 54.2-63.5%, respectively. The foregoing results concerning the compressive strengths of the mortar groups obtained in this experimental research confirms that mortars cooled in air after being exposed to applied high temperatures had higher compressive strengths compared to those cooled in water. This fact can rightfully explained by the restoration of the water ratio lost by the samples in the cooling regime application. In their experiments, previous researchers [70-71] obtained comparable results, and claimed the foregoing assertion.

With three different concentrations, 72 hours of thermal curing at 85°C, geopolymer samples exhibited the best compressive strength at 200°C. The samples of S4 group had the maximum compressive strength value when cooled in air and water after the application of 200 °C, while the samples of the reference group had the lowest strength value. Contrary to concentration of 8M with 10M concentration and subjecting to air cooling regime after applying 400°C temperature, all samples with silica fume experienced a compressive strength increase, whereas the samples of the reference group experienced a compressive strength loss. With 12M concentration, while compressive strengths of all samples with silica fume increased, both in air and water cooling after applying 400°C temperature, there was a compressive strength loss in the samples of the reference group. The increase in the compressive strength can be attributed to the increase in concentration. Anuar et al. [59] reported that the geopolymers they produced with 14M concentrations had higher compressive strengths than the ones with 8M concentrations in all compressive strength measurements at the ages of 3-28 days, which is in agreement with the results reached in the present work. At 400, 600, 800, and 1000°C cooling executed both in air and water, there are losses in compressive strengths of all groups. Despite the fact that there are losses in compressive strength after high temperature and two distinct cooling regimes, the sample with the lowest strength value is the reference

sample, and the addition of silica fume contributes to the strength at high temperatures. Different researchers have reported that the high temperature resistance of the fly ash-based geopolymers is high and addition of silica fume improves their microstructure enhancing their strength and durability [72-74]. At high temperatures, unreacted precursor grains sinter and cause the matrix to density. Owing to the high temperature resistant N-A-S-H gel, no serious decrease in strength was observed up to 400°C [88]. However, porosity and dehydration occurring in the concrete structure due to the breakdown of this bond at higher temperatures caused a decrease in strength [36]

3.6. Flexural Strength Following Exposure to High Temperatures

Figure 7 depicts the flexural strengths of groups, produced with 8M, 10M, and 12M concentrations and 72 h curing period at 85°C, after cooling in air and water, each at a time, following the exposures to high temperatures of 200, 400, 600, 800, and 1000°C.

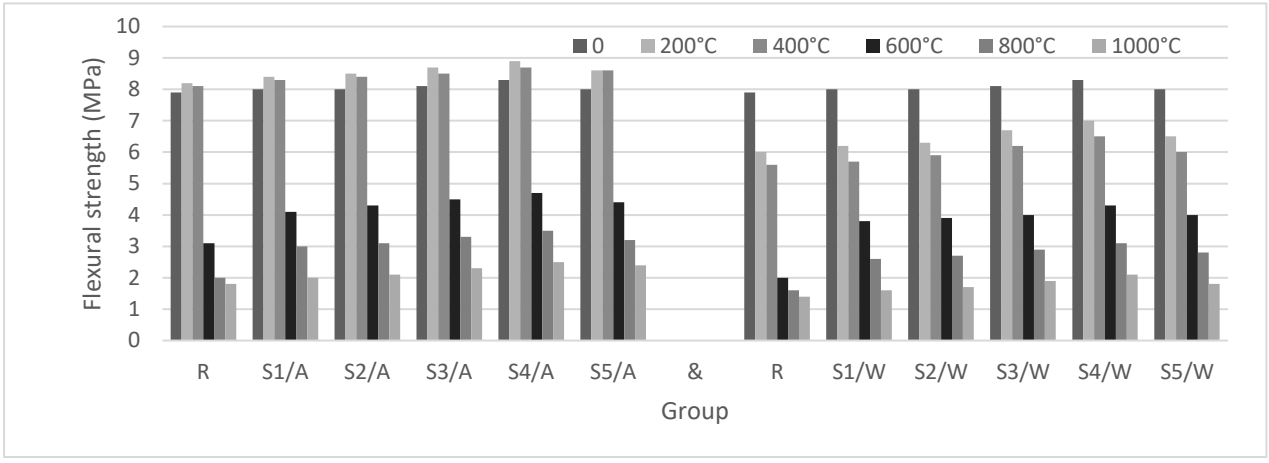

(a)

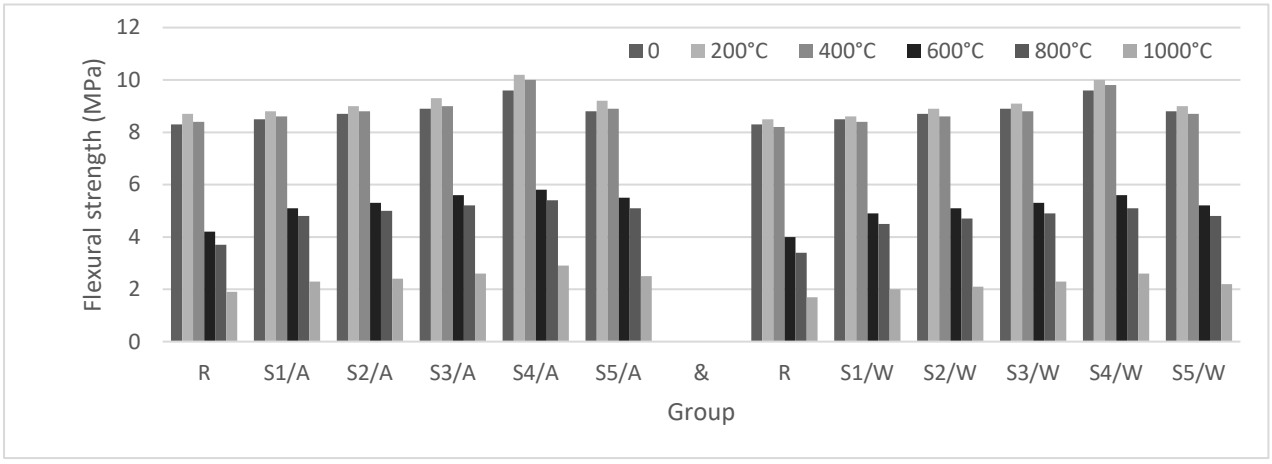

(b)

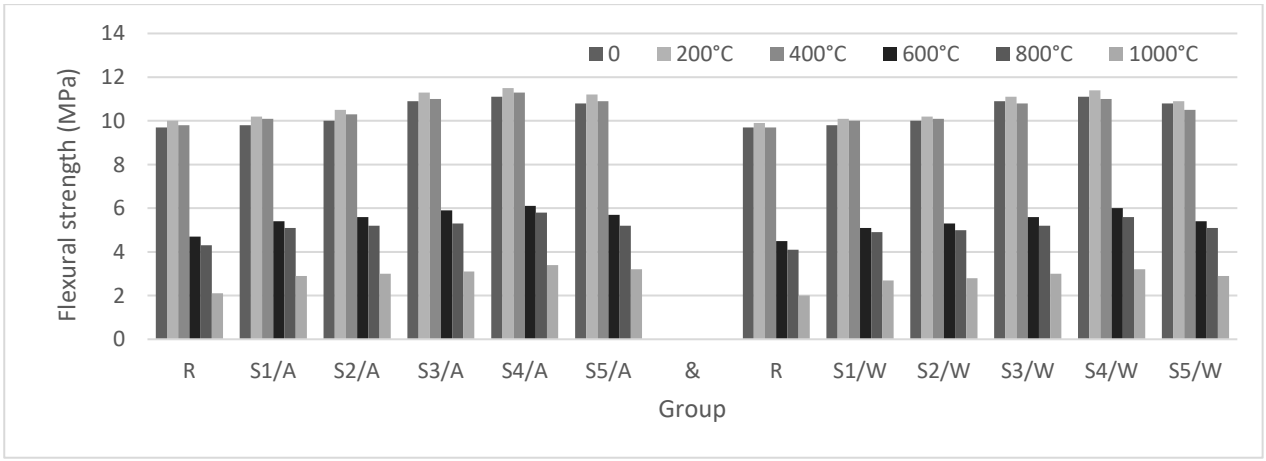

(c)

Figure 7. Residual flexural strengths of groups (a) 8M concentration (b) 10M concentration (c) 12M concentration

While examining the flexural strength values of groups with 8M concentration, it is observed that the flexural strength values following the air cooling regime after the application of 200°C are in the range 6.6-7.3 MPa, whereas the flexural strength values after the water cooling regime are in the range 6.2-7.0 MPa. After two separate cooling regimes following the application of 200°C, S4 group had the maximum flexural strength with a value of 7.9MPa, while the reference group had the lowest value with 6MPa. Following both cooling regimes after the application of 200°C Zhang [75] and Ergeshov [76] concluded that the flexural strength increased in the starting part of the interval 200-400°C and decreased in the remaining part, which is consistent with the results of the present study. This shift from increase to decrease is due to solidification in the melting process, which is corroborated by other authors, also [77-80]. The flexural strengths of groups cooled in air after being exposed to 400, 600, 800, ve 1000°C were in the ranges 8.1-8.7MPa, 4.1-4.7MPa, 3.0-3.5MPa, and 2.0-2.5MPa, respectively, and the corresponding values for groups cooled in water were in the ranges 5.7-6.5MPa, 3.8-4.3MPa, 2.6-3.1MPa, and 1,6-2.1MPa, respectively.

Among the 8M concentration groups, after the application of high temperatures of 200, 400, 600, 800 and 1000°C, the reference group yielded flexural strength values of 8.2MPa, 8.1MPa, 3.1MPa, 2MPa, and 1.8MPa, respectively, in the air cooling regime, while the corresponding values in the water cooling regime were 6MPa, 5.6MPa, 2MPa, 1.6MPa ve 1.4MPa.

When the flexural strength values of the groups with 10M concentration after the application of 200°C were examined, it was observed that the flexural strengths were in the range 8.8-10.2MPa after the air cooling regime, and in the range 8.6-10.0MPa after the water cooling regime. After both cooling regimes following the application of 200°C, flexural strength rises took place in all groups with 10M concentration. The flexural strengths of 10M concentration groups cooled in air after the application of 400, 600, 800 and 1000°C, were in the ranges 8.6-10MPa, 5.1-5.8MPa, 4.8-5.4MPa ve 2.3-2.9MPa, respectively, and the corresponding values for groups cooled in water were in the ranges 9.8-8.4MPa, 4.9-5.6MPa, 4.5-5.1MPa, and 2.1-2.6MPA, respectively. The reference group with 10M concentration cooled in air after the application of 200, 400, 600, 800 and 1000°C, acquired flexural strength values of 8.7MPa, 8.4MPa, 4.2MPa, 3.7MPa, and 1.9MPa after being exposed to high temperatures of 200-400-600-800 and 1000°C in the air cooling regime, and the corresponding values for groups cooled in water were in the ranges 8.5MPa, 8.2MPa, 4MPa, 3.4MPa ve 1.7MPa in the water cooling regime, respectively. All 10M concentration groups which were produced under identical conditions and parameters, yielded higher flexural strength values than 8M concentration groups.

Flexural strength values of the groups with 12M concentration reveals that the flexural strengths after the air cooling regime at 200 °C range from 10.2-11.5MPa, while the flexural strengths after the water cooling regime range from 10.1-11.4MPa. After varying cooling regimes at 200°C, all series exhibited pressure rises in the 8M-10M concentration range. It was discovered that the flexural strengths of samples cooled in air at 400-600-800 and 1000°C were between 10.1-11.3MPa, 5.4-6.1MPa, 5.1-5.8MPa, and 2.9-3.4MPa, respectively. The flexural strengths obtained after the water cooling regime were 10-11MPa, 5.1-6MPa, 4.9-5.6MPa, and 2.7-3.2MPa, respectively. After exposure to high temperatures of 200-400-600-800 and 1000°C, the reference sample obtained flexural strength values of 10MPa, 9.8MPa, 4.7MPa, 4.3MPa, and 2.1MPa in the air cooling regime, and 9.9 in the water cooling regime. The lowest values of strength reached were 2MPa, 9.7MPa, 4.5MPa, 4.1MPa, and 2MPa.

The maximum flexural values were found in samples cured at 12M and 85°C, as determined by an examination of the results of flexural value measurements. Abdulkarem et al. [81] reported that the strength of geopolymers at 200°C and higher decreases due to voids caused by water loss, and that the resistance to high temperature will increase by curing samples exposed to high temperature at 60-90°C. This interpretation was supported by similar findings in the study. Despite a loss in flexural strength at 600 and 1000°C, it was revealed that samples containing silica fume were more resistant to high temperatures than the control sample. Dehydration of geopolymers, evaporation, and thermal reactions are cited as the causes of the strength losses that occur at temperatures of 600 °C and above [82]. In a different study, it was reported that geopolymer mortars lost strength at high temperatures of 300-700 °C due to mass loss due to dehydraxylation cracks resulting from thermal incompatibilities, and microstructure damage [75]. In addition, the fact that the strength losses that result from flexural strength are greater than the compressive strength values can be attributed to the spreading of cracks formed at high temperatures and the fact that internal structure deterioration is more sensitive to flexural strength values [83]. According to another study, substituting silica fume for a mineral addition in the production of fly ash-based geopolymers increases their resistance to high temperatures [84]. The test data indicate that shrinkage and cracks have occurred in the samples after exposure to high temperatures, however the compressive strength losses owing to shrinkage and cracks in samples containing silica fume are minimal. In the investigation, it was determined that the mixing ratio of the S4-coded sample is optimal and that it should be utilized with high-temperature resistance.

3.7. SEM Images

Figure 8 depicts the scanning electron microscopy (SEM) images of the mortar samples which have been exposed to high temperatures.

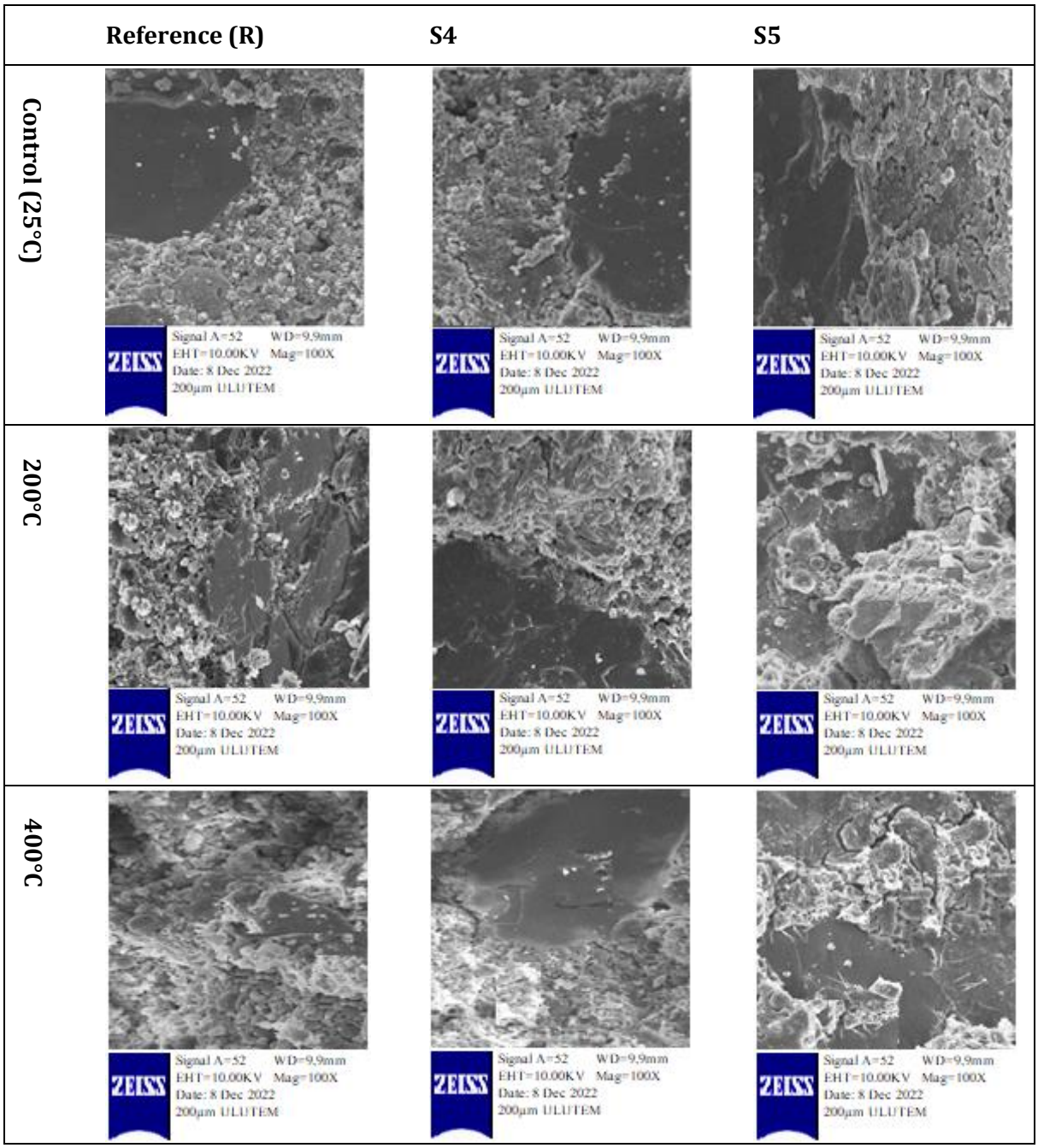

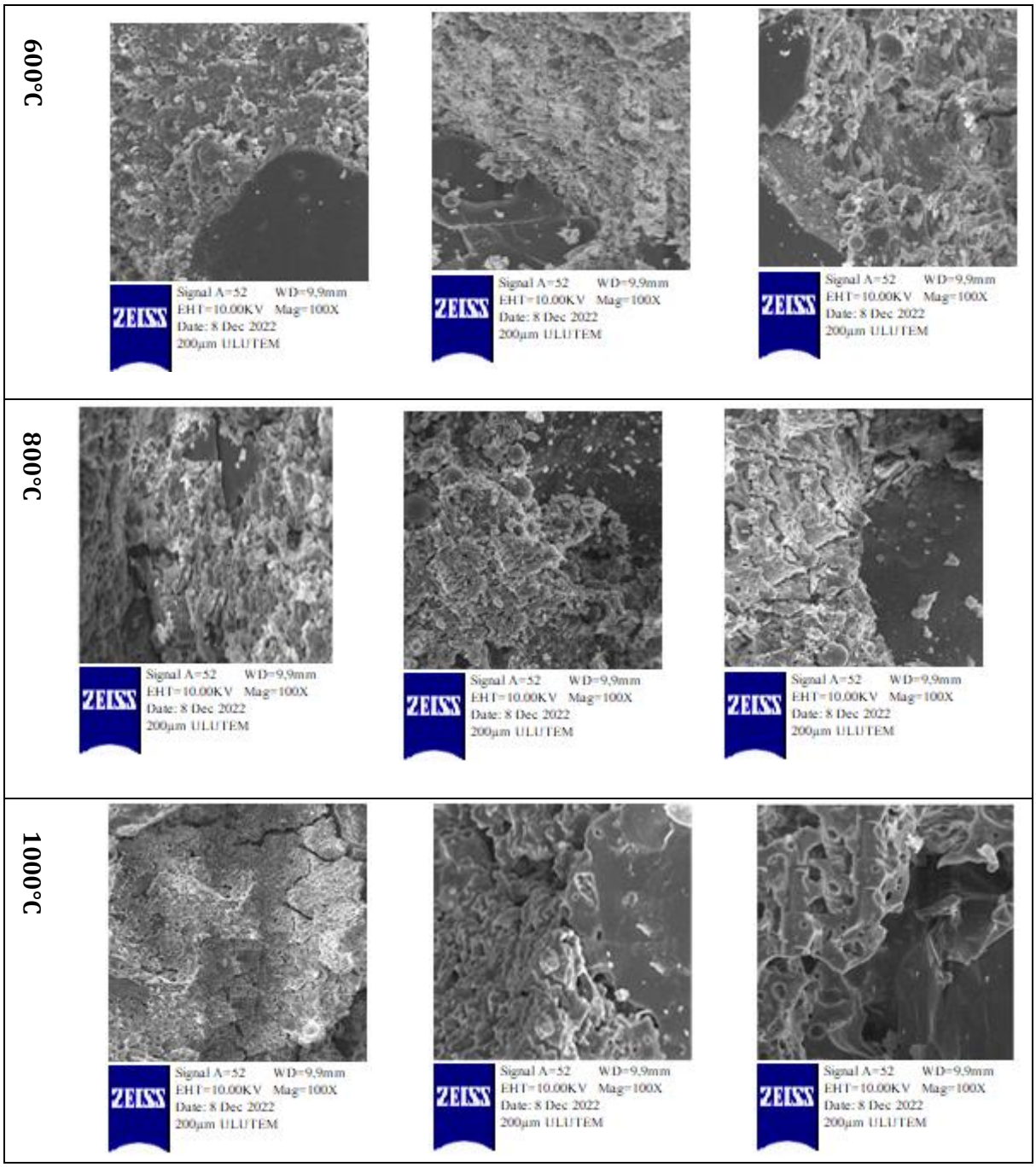

Figure 8. SEM images of R, S4 and S5 samples after being exposed to high temperatures

At temperatures between 200°C and 400°C, a geopolymer formation with a dense gel structure was found in the fly ash-based silica fume-doped S4, S5 and reference samples. This observational conclusion is consistent with the mechanical outcomes as well. In addition, no unreacted fly ash granules were seen in the SEM pictures. At temperatures of 400°C and above, the gel structure of samples S4, S5 and reference samples deteriorate and microcracks develop. Macro cracks were observed in the S5 group of samples, particularly at temperatures exceeding 600°C. The poor performance of the mechanical properties of the samples at these temperatures is concluded to be the result of microstructure degradation. SEM images of 800°C and 1000°C samples reveals the increase in the number of micro-macro cracks and the dimensions of the voids in the S4, S5 and reference samples. According to Topal et al. [42], the microstructure of geopolymers deteriorates at temperatures exceeding 200°C, resulting in a decrease in strength. According to Lahoti et al. [85], geopolymers undergo thermal contraction and expansion during exposure to high temperatures, resulting in contractions, expansions, and macro fractures. The analysis of the present study diagnosed a correlation between the cited scientific causes and the strength losses which took place in the geopolymers produced in the study.

4. Conclusion

The behavior of geopolymer samples containing fly ash-based silica fume following exposure to varied concentrations, curing durations, and temperatures was examined. The obtained results are summarized below.

- In terms of the machinability of the geopolymer samples, a diameter of 123 mm was obtained for the reference group at a concentration of 12M, whereas a diameter of 135 mm was found for the S5 group samples. The addition of silica fume and raising the concentration contributed to the machinability, as demonstrated by the results.
- When the compressive strength values of the samples were investigated, the S4 group samples with 12M concentration with a curing period of 72h at 85°C, had the highest compressive strength value of 72.3MPa. The reference group exhibited the lowest compressive strength of 64.9MPa. The addition of silica fume to the mixtures increased the values of compressive strength by up to 4%.
- The flexural strengths of the geopolymer samples were comparable to the compressive strengths. The correlation coefficient R = 0.91 supports the foregoing interpretation. The S4 group samples with 12M concentration and 72h curing at 85°C exhibited the highest flexural strength with 11.1MPa, whereas the reference group samples exhibited the lowest flexural strength under the same conditions.
- Abrasion resistances were obtained by measuring weights and volumetric losses. The S4 group samples with 12M concentration and 72h curing at 85°C demonstrated the maximum abrasion resistance with a volumetric loss of $3348mm^3/5000mm^2$ and a weight loss of 7.38 gr.
- High-temperature compressive strength values of samples produced with 12M concentration and 72h curing at 85°C were subjected to air and water cooling regimes after the applications of 200, 400, 600, 800, and 1000°C, and their high-temperature performances were assessed. While the compressive strength of the samples cooled in air increased up to 200°C, the strength of the samples decreased at 400°C and above. At temperatures as high as 400°C, the compressive strength of samples cooled in water rose, but at a slower rate than those cooled in air. The rate of strength loss is shown to rise in both cooling regimes at temperatures exceeding 400°C. At 1000°C, the compressive strengths of samples cooled in air and water are in the ranges 4.2-13.7MPa and 3.6-5.5MPa, respectively, while the compressive strengths of the reference group samples are in the ranges 2.7MPa-2.3MPa.
- In SEM analyses, it was seen that the values obtained during the determination of mechanical properties were supported. The addition of silica fume at low temperatures led to improvements in the structure of the dough. At temperatures 600°C above, the loss of strength, especially, in the S5 and reference group samples is attributed to structural flaws, macrocrack formation, and microstructure degradation. In identifying the optimal ratio of silica fume to be added to the mixture and in the interpretation of strength and durability performances, SEM, which is related to cracks, voids, and microstructure deterioration, has the potential to provide support.

Particularly the behavior of mortar after exposure to high temperatures presents significant durability issues. If it is accepted that the reliability of structures for living creatures and the economy depends on their service life, then it is impossible to describe the reliability of structures without mentioning their resistance to high temperatures. The most frequent pozzolanic materials include fly ash and silica fume, etc. As a result of the pozzolanic qualities of the materials and the incorporation of each of them into the mixture, a number of superior examples are produced. When researchers compare samples made with fly ash and silica fume to samples made without additions, a difference develops and it is possible to produce samples with higher strength and durability. It has been reported that their thermal stability is maintained even at high temperatures, such as 1200-1400°C [5, 8, 85]. Strength values of the geopolymer samples containing fly ash and silica fume utilized in the study revealed that they were resistant to high temperatures. In addition, geopolymer binders can be an alternative for the economy of fly ash and silica fume, which are produced in large amounts as waste in Turkey.

Acknowledgement

I sincerely thank the editor and reviewers for their diligent efforts in enhancing our manuscript. Their valuable contributions and commitment to excellence have greatly improved the quality and clarity of our work. We are immensely grateful for their insightful comments, constructive feedback, and meticulous attention to detail. Their support and guidance throughout this process have been invaluable.

Funding

This work with project code 2019/4-12M is supported by Kahramanmaras Sutcu Imam University Scientific Research Project Coordination Unit.

Author contributions

Ela B. Gorur Avsaroglu: Methodology, Investigation, Resources, Project administration, Writing - original draft, Writing - reviewing & editing. **Mustafa Eken:** Investigation, SEM analysis and interpretation, Writing - original draft, Writing - reviewing & editing. **Emre Eser:** Investigation, Resources.

Conflicts of interest

The authors declare no conflicts of interest.

References

1. Li, H.X., Jiang, Z.W., Yang, X.J., Yu, L., Zhang, G.F., Wu, J.G. & Liu, X.Y., (2015). Sustainable resource opportunity for cane molasses: use of cane molasses as a grinding aid in the production of Portland cement, Journal of Cleaner Production, 93, 56-64. https://doi.org/10.1016/j.jclepro.2015.01.027
2. Qu, C., Qin, Y. & Wang, T., (2024). From cement to geopoymers: Performances and sustainability advantages and sustainabiklity advantages of ambient curing, Journal of Building Engineering, 91, 109555. https://doi.org/10.1016/j.jobe.2024.109555
3. Aliabdo, A.A., Elmoaty, Abd M. & Emam, M.A., (2019). Factors affecting the mechanical properties of alkali-activated ground granulated blast furnace slag concrete, Construction and Building Materials, 197, p.p. 339–355. https://doi.org/10.1016/j.conbuildmat.2018.11.086
4. Ilcan, H., Demirbaş, A. O. Ulugöl, H. & Sahmaran. M., (2024). Low-alkaline activated construction and demolition waste-based geoplymers, Construction and Building Materials, 411, 134546. https://doi.org/10.1016/j.conbuildmat.2023.134546
5. Davidovits, J., (1994). Properties of geopolymers cements, in: P. Krivenko (Ed.), Proceedings of First International Conference on Alkaline Cements and Concretes, pp. 131–149 Kiev, Ukraine.
6. Acar, C. A., Celik, A. I., Kayabasi, R., Sener, A., Ozdoner, N. & Ozkilic, Y. O., (2023). Production of perlite-based-aerated geoplymer using hydrogen peroxide as eco-friendly material for energy-efficient buildings, Journal of Materials Research and Technology, 24, 81-99. https://doi.org/10.1016/j.jmrt.2023.02.179
7. Luna-Galiano, Y., Fernandez Pereira, C. & Vale, J., (2011). Stabilization/solidification of a municipal solid waste incineration residue using fly ash-based geopolymers, Journal of Hazardous Materials, 185 (1), 373–381. https://doi.org/10.1016/j.jhazmat.2010.08.127
8. Davidovits, J., (1991). Geopolymer, Inorganic polymeric new materials, J. Therm. Anal. Calorim. 37, 1633–1656.
9. Meskhi B., Beskopylny A. N., Stel'makh S. A., Shcherban' E. M., Mailyan L. R., Shilov A. A., El'shaeva D., Shilova K., Karalar M. & Aksoylu C., (2023). Analytical Review of Geopolymer Concrete: Retrospective and Current Issues. Materials., 16(10), 3792. https://doi.org/10.3390/ma16103792.
10. Tanan Chub-uppakarn, T., Chompoorat, T., Thepumong T., Sae-Long, W., Khamplod, A. & Chaiprapat, S. (2023). Influence of partial substitution of metakaolin by palm oil fuel ash and alumina waste ash on compressive strength and microstructure in metakaolin-based geopolymer mortar, Case Studies in Construction Materials, 19, e02519. https://doi.org/10.1016/j.cscm.2023.e02519.
11. Luna-Galiano, Y., Leiva, C., Arenas, C., Arroyo, F., Vilches, L.F., Fernández Pereira & Villegas, C., R., (2017). Behaviour of fly ash-based geopolymer panels under fire, Waste. Biomass. Valor. 8 (7), 2485–2494, https://doi.org/10.1007/s12649-016- 9803.
12. Borges P.H.R., Banthia N., & Alcamand H.A., et al. (2016). Performance of Blended Metakaolin/Blastfurnace Slag Alkaliactivated Mortars. Cement Concrete Composites, 71, 42–52. https://doi.org/10.1016/j.cemconcomp.2016.04.008
13. Fan F, Liu Z, Xu G, Peng, H. & Cai, C. S. (2018). Mechanical and thermal properties of fly ash based geopolymers. Construction and Building Materials, 160, 66–81. https://doi.org/10.1016/j.conbuildmat.2017.11.023
14. Kaur K, Singh J & Kaur M. (2018). Compressive strength of rice husk ash based geopolymer: The effect of alkaline activator, Construction and Building Materials, 169, 188–192. https://doi.org/10.1016/j.conbuildmat.2018.02.200
15. Okoye, F.N., Prakash, S. & Singh, N.B. (2017). Durability of fly ash based geopolymer concrete in the presence of silica fume, Journal of Cleaner Production, 149, 1062–1067. https://doi.org/10.1016/j.jclepro.2017.02.176
16. Celik, A. I., Ozkılıç, Y. O., Bahrami A. & Hakeem, I. Y. (2023). Mechanical performance of geopolymer concrete with micro silica fume and waste steel lathe scraps, Case Studies in Construction Materials, 19, e02548. https://doi.org/10.1016/j.cscm.2023.e02548.

17. Nochaiya, T., Wongkeo, W. & Chaipanich, A. (2010). Utilization of fly ash with silica fume and properties of Portland cement-fly ash-silica fume concrete, Fuel, 89 (3), 768–774. https://doi.org/10.1016/j.fuel.2009.10.003
18. Liu, J. & Wang, D. (2017). Influence of steel slag-silica fume composite mineral admixture on the properties of concrete, Powder Technology, 320, 230– 238. https://doi.org/10.1016/j.powtec.2017.07.052
19. Chindaprasirt, P., Paisitsrisawat, P. & Rattabasak, U. (2014). Strength and resistance to sulfate and sulfuric acid of ground fluidized bed combustion fly ash-silica fume alkali activated composite, Advanced Powder Technology, 25 (3), 1087–1093. https://doi.org/10.1016/j.apt.2014.02.007
20. Mijarsh, M.J.A., Johari, M.A.M. & Ahmad, Z.A. (2015). Compressive strength of treated palm oil fuel ash based geopolymer mortar containing calcium hydroxide, aluminum hydroxide and silica fume as mineral additives, Cement and Concrete Composites, 60, 65–81. https://doi.org/10.1016/j.cemconcomp.2015.02.007
21. Wang,Y & Zhao, J. (2018). Comparative study on flame retardancy of silica fume-based geopolymer activated by different activators, Journal of Alloys and Compounds, 743, 108-114. https://doi.org/10.1016/j.jallcom.2018.01.302
22. Wang, Y. & Zhao, J. (2018). Preliminary study on decanoic/palmitic eutectic mixture modified silica fume geopolymer-based coating for flame retardant plywood, Construction and Building Materials, 189, 1-7. https://doi.org/10.1016/j.conbuildmat.2018.08.205
23. Duan, P., Yan, C., Zhou, W. (2017). Compressive strength and microstructure of fly ash based geopolymer blended with silica fume under thermal cycle, Cement and Concrete Composites 78, 108-119. https://doi.org/10.1016/j.cemconcomp.2017.01.009
24. Uysal , M., Al-Mashhadani, M.M., Aygormez, Y. & Canpolat, O. (2018) Effect of using colemanite waste and silica fume as partial substitution on the performance of metakaolin-based geopolymer mortars, Construction and Building Materials,176, 271–282. https://doi.org/10.1016/j.conbuildmat.2018.05.034
25. Ekinci, E., Türkmen, I., Kantarci, F., & Karakoç, M.B. (2019). The improvement of mechanical, physical and durability characteristics of volcanic tuff based geopolymer concrete by using nano silica, micro silica and Styrene-Butadiene Latex additives at different ratios, Construction and Building Materials, 201, 257-267. https://doi.org/10.1016/j.conbuildmat.2018.12.204
26. Alanazi, H., Hu, J., & Kim, Y. (2019). Effect of slag, silica fume, and metakaolin on properties and performance of alkali-activated fly ash cured at ambient temperature, Construction and Building Materials, 197, 747-756. https://doi.org/10.1016/j.conbuildmat.2018.11.172
27. Cheah, C.B., Tan, L.E. & Ramli, M. (2019). The engineering properties and microstructure of sodium carbonate activated fly ash/slag blended mortars with silica fume, Composites Part B: Engineering 160, 558-572. https://doi.org/10.1016/j.compositesb.2018.12.056
28. Sayed, M. & Zeedan, S.R. (2012). Green binding material using alkali activated blast furnace slag with silica fume, HBRC Journal, 8 (3), 177-184. https://doi.org/10.1016/j.hbrcj.2012.10.003
29. Chindaprasirt, P., Paisitsrisawat, P. & Rattabasak, U. (2014). Strength and resistance to sulfate and sulfuric acid of ground fluidized bed combustion fly ash-silica fume alkali activated composite, Adv. Powder Technol. 25 (3), 1087-1093. https://doi.org/10.1016/j.apt.2014.02.007
30. Okoye, F.N., Durgaprasad, J. & Singh, N.B. (2016). Effect of silica fume on the mechanical properties of fly ash based-geopolymer concrete, Ceramics International, 42 (2), 3000-3006. https://doi.org/10.1016/j.ceramint.2015.10.084
31. Luhar, S., Nicolaides, D. & Luhar, I. (2021). Fire resistance behavior of geopolymer concrete: an overview, Buildings 11 (3), 82. https://doi.org/10.3390/buildings11030082
32. Srividya, T., Kannan Rajkumar, P.R., Sivasakthi, M., Sujitha, A. & R. Jeyalakshmi, (2022). A state-of-the-art on development of geopolymer concrete and its field applications, Case Studies in Construction Materials 16, e00812. https://doi.org/10.1016/j.cscm.2021.e00812
33. Guerrieri, M., Sanjayan J. & Collins, F. (2009). Residual compressive behavior of alkalia ctivated concrete exposed to elevated temperatures, Fire and Materials 33 (1), 51–62. https://doi.org/10.1002/fam.983
34. Sudarshan, M.S. & Ranganath, R.V. (2011). Properties of fly ash based geopolymer concrete exposed to sustained elevated temperatures, Advanced Materials Research, 250-253, 962-968. DOI:10.4028/www.scientific.net/AMR.250-253.962
35. Abdulkareem, O. A., Abdullah, M. M. A. B., Hussin, K., Ismail, K.N. & Binhussain, M. (2013). Mechanical and microstructural evaluations of lightweight aggregate geopolymer concrete before and after exposed to elevated temperatures, Materials 6 (10), 4450–4461. DOI:10.3390/ma6104450
36. Park, S.M., Jang, J.G., Lee, N.K. & Lee, H.K. (2016). Physicochemical properties of binder gel in alkali-activated fly ash/slag exposed to high temperatures, Cement and Concrete Research, 89, 72–79. https://doi.org/10.1016/j.cemconres.2016.08.004
37. Saavedra, W.G.V. & Guti´errez, R.M. de. (2017). Performance of geopolymer concrete composed of fly ash after exposure to elevated temperatures, Construction and Building Materials, 154, 229-235. https://doi.org/10.1016/j.conbuildmat.2017.07.208

38. Zhang, H., Li, L., Yuan, C., Wang, Q., Sarker, P.K., Shi, X. (2020). Deterioration of ambient cured and heat-cured fly ash geopolymer concrete by high temperature exposure and prediction of its residual compressive strength, Construction and Building Materials 262, 120924. https://doi.org/10.1016/j.conbuildmat.2020.120924
39. Sevinc, A.H., Durgun, M.Y. (2020). Properties of high-calcium fly ash-based geopolymer concretes improved with high-silica sources, Construction and building materials, 261, 120014. https://doi.org/10.1016/j.conbuildmat.2020.120924
40. Zhao, J., Wang, K., Wang, S., Wang, Z., Yang, Z., Shumuye, E.D. & Gong, X. (2021). Effect of elevated temperature on mechanical properties of high-volume fly ash-based geopolymer concrete, mortar and paste cured at room temperature, Polymers 13 (9), 1473. https://doi.org/10.3390/polym13091473
41. Ibraheem, M., Butt, F., Waqas, R.M., Hussain, K., Tufail, R.F., Ahmad, N., Usanova, K. & Musarat, M.A. (2021). Mechanical and microstructural characterization of quarry rock dust incorporated steel fiber reinforced geopolymer concrete and residual properties after exposure to elevated temperatures., Materials, 14 (22), 6890. https://doi.org/10.3390/ma14226890
42. Topal, O., Karakoç, M. B. & Ozcan, A. (2021). Effects of elevated temperatures on the properties of ground granulated blast furnace slag (GGBFS) based geopolymer concretes containing recycled concrete aggregate, European Journal of Environmental and Civil Engineering, 26(10), 4847–4862. https://doi.org/10.1080/19648189.2021.1871658
43. Tayeh, B.A., Zeyad, A.M., Agwa, I.S. & Amin, M. (2021). Effect of elevated temperatures on mechanical properties of lightweight geopolymer concrete, Case Studies in Construction Materials, 15, e00673. https://doi.org/10.1016/j.cscm.2021.e00673
44. Kantarci, F., Türkmen, I. & Ekinci, E. (2021). Improving elevated temperature performance of geopolymer concrete utilizing nano-silica, micro-silica and styrene-butadiene latex, Construction and Building Materials 286, 122980. https://doi.org/10.1016/j.conbuildmat.2021.122980
45. Huang, L., Liu, J.C., Cai, R. & Ye, H. (2021). Mechanical degradation of ultra-high strength alkali-activated concrete subjected to repeated loading and elevated temperatures, Cement and Concrete Composites, 121, 104083. https://doi.org/10.1016/j.cemconcomp.2021.104083
46. Memis, S. & Bilal, M.A.M. (2022). Taguchi optimization of geopolymer concrete produced with rice husk ash and ceramic dust, Environmental Science and Pollution Research 29 (11), 15876–15895. https://doi.org/10.1007/s11356-021-16869-w
47. Turkey, F. A., Beddu, S. Bt., Ahmed, A. N. & Al-Hubboubi, S. K. (2022). Effect of high temperatures on the properties of lightweight geopolymer concrete based fly ash and glass powder mixtures, Case Studies in Construction Materials, 17, e01489 https://doi.org/10.1016/j.cscm.2022.e01489
48. Bayrak, B., Alcan, H. G., Tanyıldızı, M., Kaplan, G., İpek, S., Aydın, A. C. & E. Güneyisi. (2024). Effects of silica fume and rice husk ash contents on engineering properties and high-temperature resistance of slag-based prepacked geopolymers, Journal of Building Engineering, 92, 109746 https://doi.org/10.1016/j.jobe.2024.109746
49. Gultekin, A. & Ramyar, K. (2023). Investigation of high-temperature resistance of natural pozzolan-based geopolymers produced with oven and microwave curing, Construction and Building Materials, 365, 130059 https://doi.org/10.1016/j.conbuildmat.2022.130059
50. TSE EN 450-1, Fly Ash- Used in Concrete- Part 1 Description, properties and conformity criteria, Turkish Standards Institute, Ankara, 2015.
51. TS EN 13263-1+A1, Silica Fume-Used in Concrete-Part1: Definitions, requirements and appropriate criteria, Turkish Standards Institute, Ankara, 2011.
52. TS EN 196-1, Cement Test Methods-Part 1: Determination of strength, Turkish Standards Institute, Ankara, 2016.
53. TS EN 1015-11, Masonry mortar- Test methods Chapter 11- Determination of tensile and compressive strength of hardened mortar in bending, Turkish Standards Institute, Ankara, 2020.
54. TS 2824 EN 1338, 2005. Concrete pavement blocks for flooring - Required conditions and test methods, Turkish Standards Institute, Ankara.
55. TS EN 1015-3, 2000. Masonry mortar- Test methods- Part 3: Determination of fresh mortar consistency (with spreading table), Turkish Standards Institute, Ankara.
56. Durak U., Karahan O., Uzal B.., Ilkentapar, S. & Atis, C.D., (2021). Influence of nano SiO_2 and nano $CaCO_3$ particles on strength, workability, and microstructural properties of fly ash-based geopolymer. Structural Concrete, 22 (S1), E352–E367. https://doi.org/10.1002/suco.201900479
57. Sathonsaowaphak A., Chindaprasirt P. & Pimraksa K., (2009). Workability and strength of lignite bottom ash geopolymer mortar, Journal of Hazardous Materials, 168 (1), 44–50. https://doi.org/10.1016/j.jhazmat.2009.01.120
58. Nath P & Sarker P. K. (2014). Efect of GGBFS on setting, workability and early strength properties of fy ash geopolymer concrete cured in ambient condition. Construction and Building Materials, 66, 163–171. https://doi.org/10.1016/j.conbuildmat.2014.05.080

59. Anuar, K. A., Ridzuan, A. R. M. & Ismail, S. (2011). Strength characteristics of geopolymer concrete containing recycled concrete aggregate, International Journal of Civil & Environmental Engineering, 11 (1), 59-62.
60. Mangat, P. S. & Ojedokun, O. (2018). Influence of curing on pore properties and strength of alkali activated mortars, Construction and Building Materials, 188, 337-348. https://doi.org/10.1016/j.conbuildmat.2018.07.180
61. Toniolo, N., Rincón, A., Roether, J.A., Ercole, P., Bernardo, E. & Boccaccini, A.R. (2018). Extensive reuse of soda-lime waste glass in fly ash-based geopolymers, Construction and Building Materials, 188, 1077-1084. https://doi.org/10.1016/j.conbuildmat.2018.08.096
62. Elyamany, H.E., Abd Elmoaty, A.E.M. & Elshaboury, A.M. (2018). Setting time and 7-day strength of geopolymer mortar with various binders, Construction and Building Materials, 187, 974–983. https://doi.org/10.1016/j.conbuildmat.2018.08.025
63. Ilkentapar, S., Ozsoy A., (2022). Investigation of mechanical properties, high-temperature resistance and microstructural properties of diatomite-containing geopolymer mortars, Arabian Journal of Geosciences, 15 (6), 502, https://doi.org/10.1007/s12517-022-09824-7.
64. Zannerni, G. M., Fattah, K. P. & Al-Tamimi, A. K. (2020). Ambient-cured geopolymer concrete with single alkali activator, Sustainable Materials and Technologies, 23, e00131, https://doi.org/10.1016/j.susmat.2019.e00131
65. Chindaprasirt, P., Paisitsrisawat, P. & Rattanasak, U. (2014). Strength and resistance to sulfate and sulfuric acid of ground fluidized bed combustion fly ash-silica fume alkali-Activated composite, Advanced Powder Technology, 25(3), 1087–1093. https://doi.org/10.1016/j.apt.2014.02.007
66. Hu S., Wang H., Zhang G. & Ding Q, (2008). Bonding and abrasion resistance of geopolymeric repair material made with steel slag. Cement and Concrete Composites, 30 (3), 239-244. https://doi.org/10.1016/j.cemconcomp.2007.04.004
67. Bilim C, Karahan O, Atis CD & Ilkentapar S., (2013), Influence of admixtures on the properties of alkali-activated slag mortars subjected to different curing conditions, Materials & Design, 44, 540–547. https://doi.org/10.1016/j.matdes.2012.08.049
68. Ilkentapar S, Atis C. D. , Karahan O. & Gorur Avsaroglu E. B. (2017), Influence of duration of heat curing and extra rest period after heat curing on the strength and transport characteristic of alkali activated class F fly ash geopolymer mortar, Construction and Building Materials, 151, 363–369. https://doi.org/10.1016/j.conbuildmat.2017.06.041
69. Durak U, Ilkentapar S, Karahan O, Uzal, B. &Atis, C. D., (2021). A new parameter influencing the reaction kinetics and properties of fly ash based geopolymers: a pre-rest period before heat curing, Journal of Building Engineering, 35, 102023. https://doi.org/10.1016/j.jobe.2020.102023
70. Simsek, O. (2009). "Concrete and Concrete Technology", Ankara, Seckin Publishing (3rd edition) ,161-164.
71. Bingöl, A. & Rustem, Gul, R., (2009). A Review on Reinforcement-Concrete Adherence, Effects of High Temperatures on Concrete Strength and Adherence, Tubav Journal of Science, 2(2), 211-230.
72. Wongkeo, W., Thongsanitgarn, P., Ngamjarurojana, A. & Chaipanich, A. (2014). Compressive strength and chloride resistance of self-compacting concrete containing high level fly ash and silica fume, Materials & Design, 64, 261-269. https://doi.org/10.1016/j.matdes.2014.07.042
73. Farahani, A., Taghaddos, H. & Shekarchi, M. (2015). Prediction of long-term chloride diffusion in silica fume concrete in a marine environment, Cement and Concrete Composites, 59, 10-17. https://doi.org/10.1016/j.cemconcomp.2015.03.006
74. Lilkov, V., Rostovsky, I., Petrov, O., Tzvetanova, Y. & P. Savov, (2014). Long term study of hardened cement pastes containing silica fume and fly ash, Construction and Building Materials 60, 48-56. https://doi.org/10.1016/j.conbuildmat.2014.02.045
75. Zhang, H. Y., Kodur, V., Wu, B., Cao, L. & Wang, F. (2016). Thermal behavior and mechanical properties of geopolymer mortar after exposure to elevated temperatures, Construction and Building Materials, 109, 17-24. https://doi.org/10.1016/j.conbuildmat.2016.01.043
76. Ergeshov, Z. (2021). Investigation of the effects of silica fume substitution on physical and mechanical properties of fly ash based geopolymer mortars. MSc Thesis, Erciyes University Graduate School of Natural and Applied Sciences, Department of Civil Engineering.
77. Bakharev, T., (2006). Thermal behaviour of geopolymers prepared using class F fly ash and elevated temperature curing, Cement and Concrete Research, 36 (6), 1134-1147. https://doi.org/10.1016/j.cemconres.2006.03.022
78. Barbosa, V.F.F. & Mackenzie, K.J.D. (2003). Thermal behaviour of inorganic geopolymers and composites derived from sodium polysialate, Materials Research Bulletin, 38 (2), 319–331. https://doi.org/10.1016/S0025-5408(02)01022-X
79. Skvara, F., Jilek, T. & Kopecky, L. (2005). Geopolymer materials based on fly ash, Ceramics-Silikáty, 49 (3), 195–204.

80. Krivenko, P.V. & Kovalchuk, G.Y., (2007). Directed synthesis of alkaline aluminosilicate minerals in a geocement matrix, Journal of Material Science, 42, 2944–2952. https://doi.org/10.1007/s10853-006-0528-3
81. Abdulkareem, O. A., Al Bakri, A. M., Kamarudin, H., Nizar, I. K. & Ala'eddin, A. S. (2014). Effects of elevated temperatures on the thermal behavior and mechanical performance of fly ash geopolymer paste, mortar and lightweight concrete. Construction and Building Materials, 50, 377-387. https://doi.org/10.1016/j.conbuildmat.2013.09.047
82. Zhang, Y.J., Li, S., Wang, Y.C. & Xu, D.L., (2012). "Microstructural and strength evolutions of geopolymer composite reinforced by resin exposed to elevated temperature", Journal of Non-Crystalline Solids, 358 (3), 620–624. https://doi.org/10.1016/j.jnoncrysol.2011.11.006
83. Zhang, H.Y., Kodur, V., Wu, B., Cao, L. & Qi, S.L., (2015). "Comparative thermal and mechanical performance of geopolymers derived from metakaolin and fly ash", Journal of Materials in Civil Engineering, 28(2), https://doi.org/10.1061/(ASCE)MT.1943-5533.0001359
84. Messina, F., Ferone, C., Colangelo, F. F., Roviello, G. &Cioffi, R., (2018). Alkali activated waste fly ash as sustainable composite: Influence of curing and pozzolanic admixtures on the early-age physico-mechanical properties and residual strength after exposure at elevated temperature, Composites Part B-Engineering, 132, 161-169. https://doi.org/10.1016/j.compositesb.2017.08.012
85. Lahoti M., Wong K. K., Yang E. H. & Tan K. H., (2018) Effects of Si/Al molar ratio on strength endurance and volume stability of metakaolin geopolymers subject to elevated temperature, Ceramics International, 44(5) 5726– 5734. https://doi.org/10.1016/j.ceramint.2017.12.226
86. Dehghani, A., Aslani, F. & Panah, N. G., (2021) Effects of initial SiO2/Al2O3 molar ratio and slag on fly ash-based ambient cured geopolymer properties, Construction and Building Materials, 293, https://doi.org/10.1016/j.conbuildmat.2021.123527
87. Saridemir, M. & Celikten, S., (2023), Effects of Ms modulus, Na concentration and fly ash content on properties of vapour-cured geopolymer mortars exposed to high temperatures, Construction and Building Materials, 363, https://doi.org/10.1016/j.conbuildmat.2022.129868
88. Luo, Y, Klima, K. M., Brouwers, H. J. H. & Yu, O., (2022), Effects of ladle slag on Class F fly ash geopolymer: Reaction mechanism and high temperature behavior, Cement and Concrete Composites, 129, https://doi.org/10.1016/j.cemconcomp.2022.104468Iban.